Supporting Information for

Conformal Electrocatalytic Surface Nanoionics for Accelerating High-Temperature Electrochemical Reactions in Solid Oxide Fuel Cells

Yun Chen[1], Kirk Gerdes[2], Sergio A. Paredes Navia[1], Liang Liang[1], Alec Hinerman[1], Xueyan Song[1*]

[1] Department of Mechanical & Aerospace Engineering, West Virginia University, Morgantown, WV 26506, USA

[2] U.S. DOE, National Energy Technology Laboratory, Morgantown, WV 26507, USA

* Correspondence to: Xueyan.Song@mail.wvu.edu

Experimental Section. Commercially available, anode-supported solid oxide button cells fabricated by Materials and Systems Research, Inc. (MSRI, Salt Lake City, UT) were employed for all the experiments described in this paper. MSRI cells are composed of five layers as follows, starting from the anode: ~0.9 mm thick Ni/YSZ cermet layer which supports the cell structure; 15 μm thick Ni/YSZ active layer; ~12 μm thick YSZ electrolyte; ~15 μm thick $La_{0.8}Sr_{0.2}MnO_3$ / 8YSZ active layer; and 50 μm thick, pure LSM current collecting layer. The cell active area (limited by the cathode) is 2 cm^2. The exposure area of the anode to fuel is about 3.5 cm^2.

The ALD coatings were performed in a commercial GEMStar-8 ALD reactor from Arradiance Inc. The precursors used in this study were all purchased from Strem Chemicals, Inc. The (trimethyl)methylcyclopentadienylplatinum(IV), (99 %) and the deionized water were used as Pt precursor and oxidant for depositing Pt layer; and the bis(cyclopentadienyl)manganese (98+ %), the bis(cyclopentadienyl)cobalt (II), (min. 98 % cobaltocene) and ozone were used as Mn, Co, and oxidant, respectively, for $(Mn_{0.8}Co_{0.2})O_x$ layer growth. During the deposition, the (trimethyl)methylcyclopentadienylplatinum, bis(cyclopentadienyl)manganese, and bis(cyclopentadienyl)cobalt containers were maintained at 75 ºC, 90 ºC and 90 ºC, respectively; and the reactor chamber was set at 300 ºC. Total 100 cycles were performed for each element deposition, leading to a dual-layer ALD coating of ~ 3 nm Pt first, followed by ~10 nm $(MnCo)_3O_4$ layer (consisting 8 nm Mn_3O_4 and 2 nm of Co_3O_4) as schematically shown in **Figure S1**.

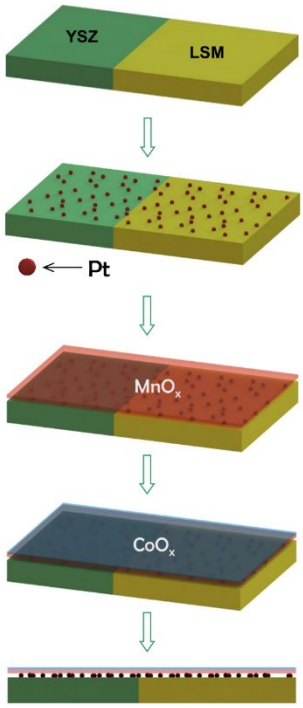

Figure S1 Schematic of ALD deposition procedure.

This is simple one-step processing of as-received cells, and the change of the chemistry in the ALD layer was achieved through computer-controlled automatic switching of the precursors. No surface pretreatment was applied to the cells, and no heat-treatment was applied before or after ALD coating either. The cell electrochemical operation was carried out directly after the ALD coating.

All cell tests were performed on a test stand. The platinum mesh was used for anode and cathode lead connections. The fuel and air stream flow rates were controlled separately using mass flow controllers. Cell testing was performed at 750 ºC. During the operation, a 600 mL/min air flow rate and a 600 mL/min fuel flow rate were used. Before any electrochemical measurements, all cells were current-treated for approximately 16 h under a small current density of 0.1 A/cm^2 to ensure they were activated. After that, all samples were loaded at a constant current of 0.3 A/cm^2 for desired periods. The cell performance was examined using a TrueData-load modular electronic dc load which guarantees voltage and current accuracies of 0.03 % FS of the range selected +/- 0.05% of the value. The cell impedance spectra were examined using a potentiostat/galcanostat (Solartron 1287A) equipped with a frequency response analyzer (Solartron 1260). All data reported in **Table 1** were taken after the current treat for comparison. Impedance measurements were carried out using a Solatron 1260 frequency response analyzer in a frequency range from 50 MHz to 100 kHz. The impedance spectra and resistance (R_s and R_p) presented are those measured under a DC bias current of 0.3 A/cm^2. On a Nyquist plot, R_s is determined by the intercept at the higher

frequency end and R_p is determined by the distance between two intercepts.

ALD coated cells were sectioned and subjected to nanostructural and crystallographic examination using high resolution (HR) Transmission Electron Microscopy (TEM). All the TEM examinations were conducted in the cathode active layer. TEM samples were prepared by mechanical polishing and ion milling in a liquid-nitrogen-cooled holder. Electron diffraction, diffraction contrast, and HRTEM imaging were performed using a JEM-2100 operated at 200 kV. Chemical analysis was carried out under TEM using energy dispersive X-ray Spectroscopy (EDS).

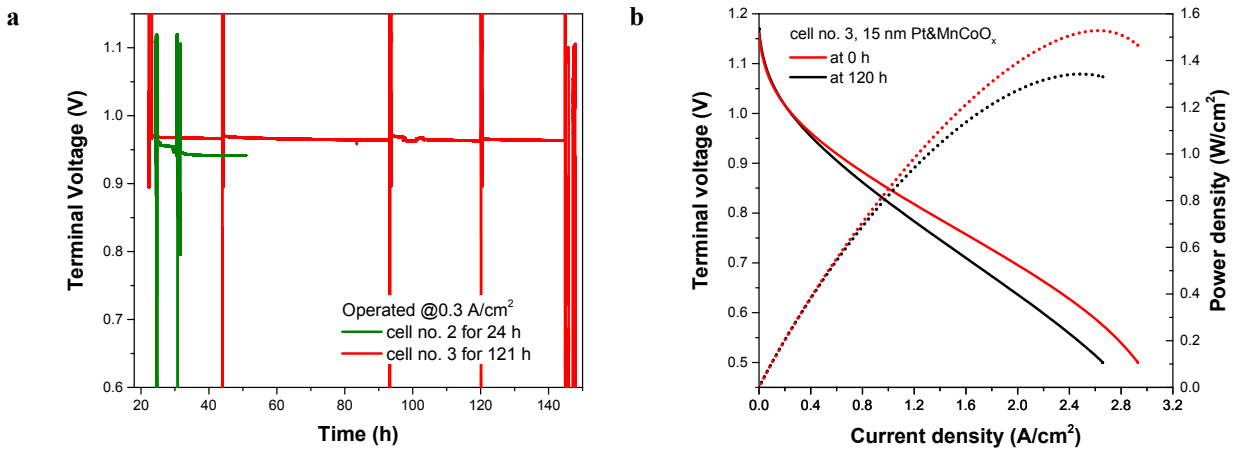

Figure S2 **a**, Terminal voltage of cell no. 2 with Pt and 5 nm $(Mn_{0.8}Co_{0.2})_3O_4$ layer and cell no. 3 with Pt and 15 nm $(Mn_{0.8}Co_{0.2})_3O_4$ layer as a function of operating time at a constant current density of 0.3 A/cm^2 at 750 °C. **b**, Terminal voltage and power density as a function of current density for cell no. 3 at 0 h and 120 h operation.

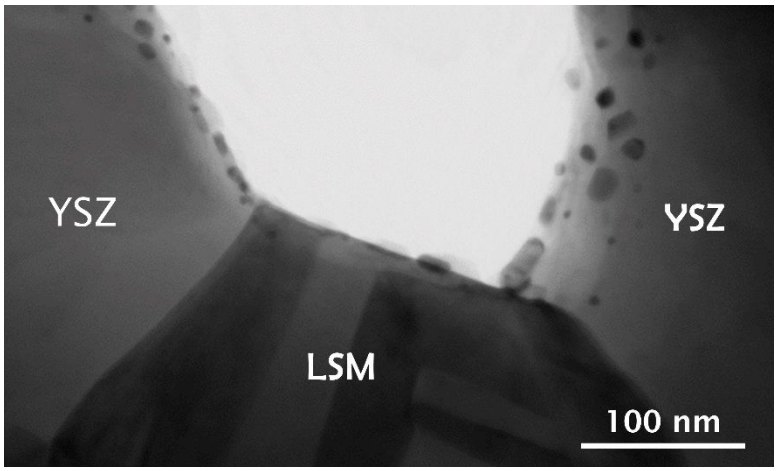

Figure S3 The enlarged view of Figure 2f showing that surface of LSM surface of Cell no. 2 is mostly free of Pt particles.

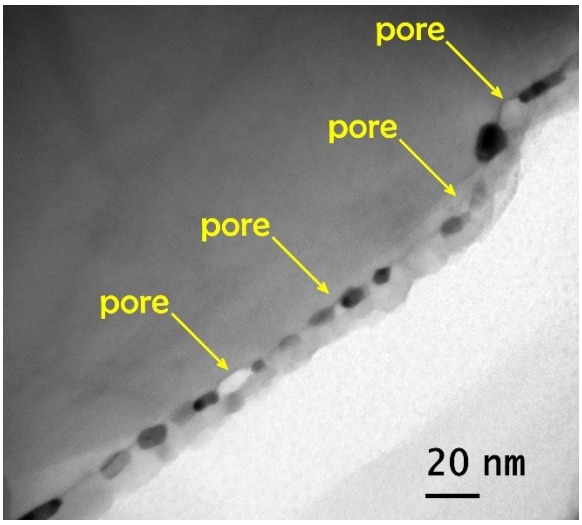

Figure S4 Nano-pores are present in the operated cell no. 3 with Pt and 15 nm $(Mn_{0.8}Co_{0.2})_3O_4$ layer.

In order to support the discussion of the electrical oxide conductor $(Mn_{0.8}Co_{0.2})_3O_4$ possessing substantial ionic conductivity, we have conducted synthesis and conductivity measurement of $(Mn_{0.8}Co_{0.2})_3O_4$ pellet sample.

In detail, $(Mn_{0.8}Co_{0.2})_3O_4$ powders were prepared by the sol-gel route. $Mn(NO_3)_2{\cdot}4H_2O$ (Manganese nitrate), and $Co(NO_3)_2{\cdot}6H_2O$ (Cobalt nitrate) were mixed in stoichiometric ratios in deionized water. Ethylene glycol and polyethylene glycol were used to polymerize the solution. Nitric acid was added to induce the decomposition of nitrate salts and facilitate the formation of a new compound. The mix was mechanically stirred at 85 °C for 3 h to form a gel. The gel was ashed at 500 °C for 2 h in a box furnace. The ashed product was planetary ball milled in ethyl alcohol for 10 min. The milled powder was calcined at 700 °C for 2 h in a tube furnace with 5 % oxygen balance nitrogen flow. The resultant powder was then uniaxially pressed into 13 mm pellets (1 g) under 1 GPa for 10 min at 25 °C. The pellets were then sintered at 750 °C for 2 h, in a tube furnace with 5 % oxygen balance nitrogen flow, and the pellets are with the grain size of ~ 200 nm.

After sintering, the samples were cut into the rectangular shape and subject to electronic-ionic conductivity measurement. The four-point conductivity measurement was conducted at 650 ºC, 750 ºC, 800 ºC and 850 ºC in the air using Au paste and Au wires for lead connection. For examining the ionic component of the conductivity of the mixed conductor sample, the Hebb-Wagner polarization method [1,2,3] was employed. In particular, a commercial 8YSZ was used as a blocking material to filter the electronic component during the measurement.

Table S1 Total and the ionic conductivity of $(Mn_{0.8}Co_{0.2})_3O_4$ samples. Literature data of the ionic conductivity for YSZ, LSCF, and SDC are listed for comparison.

Material	Total conductivity (S cm^{-1})		Ionic conductivity (S cm^{-1})		References
	750 °C	800 °C	750 °C	800 °C	
$(Mn_{0.8}Co_{0.2})_3O_4$	0.311	0.571	0.006	0.017	
YSZ	-	-	0.027	0.044	4
	-	-	0.021	0.032	5
LSCF	345	318	-	-	6
	375	333	0.041	0.078	7
SDC	-	-	0.033	0.054	8

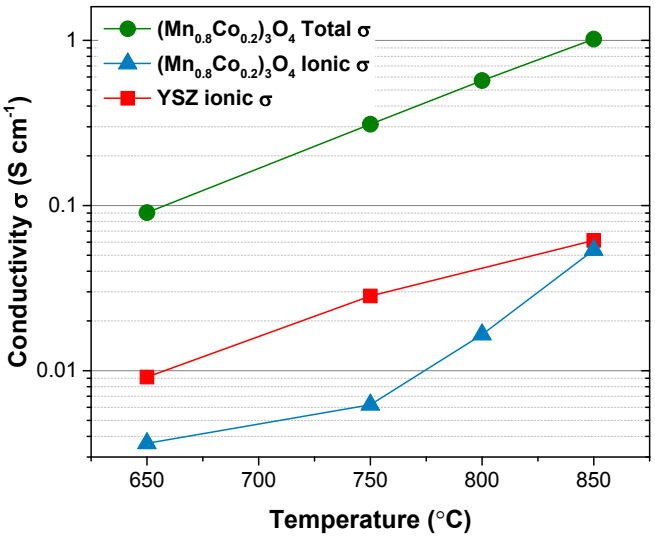

Figure S5 Total and ionic conductivity of $(Mn_{0.8}Co_{0.2})_3O_4$ samples. Literature data of the ionic conductivity for YSZ are plotted for comparison.

Reference

1 Riess, I. *Solid State Ionics* **1996,** 91, 221-232.

2 Riess, I. *Solid State Ionics* **1992,** 51, (3-4), 219-229.

3 Miruszewski, T.; Karczewski, J.; Bochentyn, B.; Jasinski, P.; Gazda, M.; Kusz, B. *Journal of Physics and Chemistry of Solids* **2016,** 91, 163-169.

4 Joo, J. H.; Choi, G. M. *Solid State Ionics* **2006,** 177, 1053-1057.

5 Zink, P. A.; Yoon, K. J.; Pal, U. B.; Gopalan, S. **2009,** 12, B141-B143.

6 Stevenson, J.; Armstrong, T.; Carneim, R.; Pederson, L.; Weber, W. *Journal of the Electrochemical Society* **1996,** 143, 2722-2729.

7 Kostogloudis, G. C.; Ftikos, C. *Solid State Ionics* **1999,** 126, 143-151.

8 Hua, G.; Ding, X.; Zhu, W.; Li, J. *Journal of Materials Science: Materials in Electronics* **2015,** 26, 3664-3669.